



BNL-203433-2018-JAAM

A comprehensive study of catalytic, morphological and electronic properties of ligand-protected gold nanoclusters using XPS, STM, XAFS, and TPD techniques

Q. Wu, X. Tong

To be published in "Royal Society of Chemistry"

December 2017

Center for Functional Nanomaterials
Brookhaven National Laboratory

U.S. Department of Energy
USDOE Office of Science (SC), Basic Energy Sciences (BES) (SC-22)

Notice: This manuscript has been authored by employees of Brookhaven Science Associates, LLC under Contract No. DE-SC0012704 with the U.S. Department of Energy. The publisher by accepting the manuscript for publication acknowledges that the United States Government retains a non-exclusive, paid-up, irrevocable, world-wide license to publish or reproduce the published form of this manuscript, or allow others to do so, for United States Government purposes.

DISCLAIMER

This report was prepared as an account of work sponsored by an agency of the United States Government. Neither the United States Government nor any agency thereof, nor any of their employees, nor any of their contractors, subcontractors, or their employees, makes any warranty, express or implied, or assumes any legal liability or responsibility for the accuracy, completeness, or any third party's use or the results of such use of any information, apparatus, product, or process disclosed, or represents that its use would not infringe privately owned rights. Reference herein to any specific commercial product, process, or service by trade name, trademark, manufacturer, or otherwise, does not necessarily constitute or imply its endorsement, recommendation, or favoring by the United States Government or any agency thereof or its contractors or subcontractors. The views and opinions of authors expressed herein do not necessarily state or reflect those of the United States Government or any agency thereof.

Comprehensive Study of Catalytic, Morphological and Electronic Properties of Ligand-protected Gold Nanoclusters by XPS, STM, XAFS, and TPD Techniques

Qiyuan Wu,^{a†} Jiajie Cen,^{a†} Yue Zhao,^b Xiao Tong,^c Yuanyuan Li,^a Anatoly I. Frenkel,^{a,d} Shen Zhao,^{e*} and Alexander Orlov^{a*}

Ultra small gold nanoclusters were synthesized by ligand exchange method and deposited onto different TiO_2 supports to study their properties. STM imaging revealed that the as-synthesized gold nanoclusters had 2-D morphology consisting of monolayer of gold atoms. Subsequent XPS, XAFS, and CO oxidation TPD results indicated that heat treatments of gold clusters at different temperatures significantly altered their electronic and catalytic properties due to ligand deprotection and cluster agglomeration.

Introduction

Metal nanoclusters (NCs) are very promising catalysts for a number of different applications.¹⁻⁶ For many years, bulk Au was considered to be inert and therefore ineffective material for catalytic applications. However, this notion has substantially evolved following a discovery of Au size-effect, where Au particles of few nm in size were shown to exhibit catalytic activity.⁷⁻⁹ Reducing Au size to even smaller dimensions appears to be the next logical step exploring its chemistry. It was previously reported that the catalytic activity of supported Au NCs depends on the number of Au atoms contained in the NC.¹⁰⁻¹² Therefore, a more granular knowledge on size effect of Au NCs is needed to tune their unique properties to facilitate chemical reactions.^{1, 13-23} In addition to size, a geometry of these NCs may prove to be another important parameter to tune their properties, given that coordination of Au atoms and NCs electronic structure are shape dependent, especially for sub-nm dimensions^{24, 25} It is also important to note that the shape of supported NCs is often overlooked parameter in the published literature, where the NCs size is used as a primary factor to explain their catalytic activity. Unfortunately, despite impressive advances in microscopy techniques, a reliable determination of Au NCs shape as size-averaged parameter still remains challenging.^{22, 26, 27}

In addition to describing challenges in NCs characterization, it is also important to outline different approaches to their synthesis^{1, 11, 28-32} Among several synthetic methods, size-selected cluster (SSC) approach is the one providing a very good control of cluster size, while producing extremely clean NCs under the ultra-high vacuum (UHV) conditions. Importantly, this approach has advantage over other methods of NCs synthesis, given that the clusters produced by SSC method can be characterized *in-situ* during the synthesis.^{33, 34} Size selected approach also has disadvantages as compared to more traditional chemical synthesis methods. For example, SSC method is regarded as being much less scalable and more difficult to use for NCs deposition onto complex three dimensional substrates as compared to the alternative methods. In addition to consideration of cluster size, it is also important to highlight the effect of surface modification on catalytic activity. The synthetic methods achieving good control of cluster size often utilize ligands or surfactants to control the size of clusters during chemical synthesis of NCs. Such control of cluster size also has notable disadvantages as ligands and surfactants can block active sites on supported NCs surfaces, thereby requiring additional treatment to activate them for catalytic applications. Therefore, developing scalable methods of NCs synthesis, while understanding and optimizing both cluster size and surface coverage/deprotection, is an important topic of research.

In this work, Au NCs were synthesized by ligand exchange method using diphosphine ligands and deposited onto both TiO_2 single crystal and powder supports to understand their behavior in model and practical catalytic systems. The supported Au NCs were subjected to heat treatment at different temperatures based on published protocol for activation of supported ligand-protected Au clusters.^{16, 35-37} The Au NCs supported on single crystals were imaged by scanning tunneling microscope (STM). Additionally, X-ray photoelectron spectroscopy (XPS), temperature-programmed desorption

^a Department of Material Science and Chemical Engineering, Stony Brook University, Stony Brook, NY 11794, USA.

^b Department of Chemistry, Stony Brook University, Stony Brook, NY 11794, USA.

^c Center for Functional Nanomaterials, Brookhaven National Laboratory, Upton, NY 11973, USA.

^d Division of Chemistry, Brookhaven National Laboratory, Upton, NY 11973, USA

^e Energy and Environment Research, Southern Research, Durham, NC 27712, USA

*Email: alexander.orlov@stonybrook.edu

*Email: silaszho@gmail.com

†equal contribution

Electronic Supplementary Information (ESI) available: supporting figures and table.

See DOI: 10.1039/x0xx00000x

(TPD) for CO oxidation, and *in-situ* X-ray absorption fine structure (XAFS) spectroscopy including both X-ray absorption near edge structure (XANES) and extended X-ray absorption fine structure (EXAFS) spectroscopies, were utilized to examine the evolution of Au NCs as a function of temperature. The novelty of this work is in both utilization of distinct ligand-protected clusters coupled with comprehensive elucidation of their properties using a combination of microscopy and spectroscopy techniques.

Experimental

Synthesis and deposition of Au NCs. Au NCs were synthesized following procedures developed in our group, which were based on modification of the previously published ligand exchange approach.^{2, 3, 31} Briefly, Au(PPh₃)Cl was dissolved in CHCl₃ to reach a final concentration of 10⁻³ mol/L. About 10⁻³ mol/L P(PPh₂)₂(CH₂)₄P(PPh₂) was then added to the mixture to achieve the target cluster size. Finally, 5 × 10⁻³ mol/L of the reducing agent (NaBH₄) was added under continuous stirring for 24 hours at room temperature to produce the Au NCs suspension. The as-synthesized Au NCs suspension was characterized by UV-Visible spectroscopy (Thermo Evolution 300) and matrix-assisted laser desorption / ionization – time of flight mass spectroscopy (MALDI-TOF MS, Bruker AutoFlexII system). To deposit Au NCs onto TiO₂ single crystal (rutile, 110), the Au NCs suspension was transferred to a manifold and degassed. The manifold was then connected to the load lock chamber of UHV system. Deposition was controlled through an electromagnetic pulse valve (Parker). To deposit 2.5 wt% Au NCs onto TiO₂ (rutile) powders, about 200 mg TiO₂ was added to 20 mL of dichloromethane, followed by addition of Au NCs suspension. The mixture was then stirred overnight to evaporate the solvent.

UHV experiment. STM imaging was carried out using RHK STM 5000 microscope operating in constant current mode. TiO₂ single crystal was first treated according to an Ar⁺ sputtering-annealing cleaning procedure to reach atomically flat and clean surfaces, as confirmed by STM images. Au NCs were then deposited onto the TiO₂ single crystal located in the load lock chamber via an electromagnetic pulse valve (Parker). After the deposition, the Au NCs modified TiO₂ single crystal was again imaged by the STM. After heating the sample at different temperatures (300 K, 373 K, 423 K, and 523 K) for 30 min, the surfaces were characterized by XPS and TPD. XPS measurements were done by hemispherical electron energy analyzer with X-rays generated by non-monochromatic Al K α (1486.6 eV) source. Analysis of the XPS spectra was performed using XPSPEAK version 4.1 software. The Ti 2p_{3/2} signal at 458.5 eV was used to calibrate the energy scale to which all the measured binding energies were adjusted, with Shirley background applied to all spectra. ¹³C labeled ¹³CO was used in TPD experiment in order to exclude the interference of CO₂ present in the chamber, which also include CO₂ originated from oxidation of surface contaminants. The TPD experiment was conducted as following: firstly, the sample was cooled to 90 K by liquid N₂; then O₂ was dosed at 10⁻⁵ torr and 90 K for 15

minutes following by the sample exposure to ¹³CO at 4×10⁻⁵ torr for 15 minutes. Large exposure of gases was performed here in order to ensure the saturation coverage. Meanwhile, it has been shown that, for Au catalyst for CO oxidation reaction, the order of exposure of reactant gases does not change the activity.³² The sample was then heated to different target temperatures at a ramping rate of 30 K/min. The upper temperature for the TPR experiment was set to be equal to the heat treatment temperature. The rational for such temperature selection was based on consideration of NCs stability during the CO oxidation experiment. During the TPD experiment, desorbed species were detected by a quadrupole mass spectrometer (MS). Measurements of catalytically produced ¹³CO₂ were based on “m/e = 45” signal.

In-situ XANES measurement. *In-situ* XAS measurements were performed at Beamline X18B (NSLS, Brookhaven National Laboratory). The Au L₃ edge spectra of 2.5 wt% Au/TiO₂ catalysts were collected in fluorescence mode. The sample powders were pressed into pellets and mounted into a custom-designed and - built catalyst cell. Subsequently, He gas was introduced to the cell by mass flow controller. Spectra were collected upon different heat treatment.

Results and discussion

Figure 1a shows STM image of clean TiO₂ (110)-(1×1) surface. The image indicates a presence of terraces with width of a few hundred Å and steps with height of ~ 3 Å, which is consistent with the expected step height for rutile (110)-(1×1) surface described in literature.^{34, 38} Figure 1b shows STM image of clean TiO₂ surface at higher magnification. The alternating bright and dark lines corresponds to 5-fold coordinated Ti atom (5c-Ti) rows and bridging oxygen rows respectively. The separation of ~ 6.5 Å between neighboring Ti atom rows is also consistent with the published literature.^{34, 39}

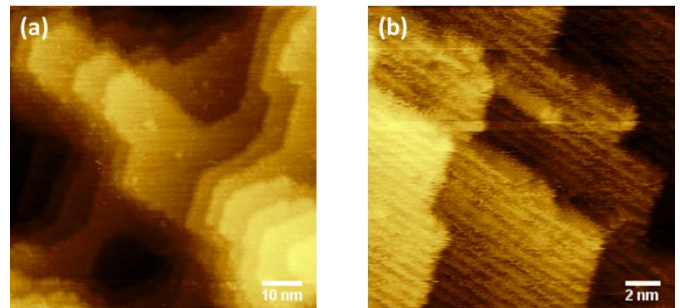


Figure 1: STM images of clean TiO₂ (110)-(1×1) surface. The alternating bright and dark lines in figure (b) corresponded to 5-fold coordinated Ti atom (5c-Ti) rows and bridging oxygen rows, respectively.

Following the imaging of TiO_2 (110)-(1×1) surface, it was modified with Au NCs, which were delivered via an electromagnetic pulse valve. Figures 2a-c show STM images of Au NCs modified TiO_2 surface at different magnifications. At low magnification (Figure 2a), Au NCs appeared as uniform particles with the width of ~ 2 nm. However, higher magnifications images (Figures 2b - 2c, and S1 in supplementary information, SI) reveal that these particles were formed from smaller Au NCs. It is worth noting that the results described above suggest that this method of deposition is promising for producing high coverage layers of small size of NCs, which is often challenging task for traditional deposition approaches. The height and width distribution of Au NCs based on Figure 2b are presented in Figure 2d. The average height and width of supported Au NCs were about 1.6 Å and 6.5 Å respectively. A typical line scan of two Au NCs is shown in Figure S2 in SI. Given these dimensions, one may conclude that the Au NCs consisted of one atomic layer of ~ 10 Au atoms. Such conclusion agrees well with our previous work showing that Au NCs synthesized by this ligand exchange approach contains 8 to 11 Au atoms.² The uniformity of synthesized Au NCs was also confirmed by UV-Visible spectroscopy and MALDI-TOF mass spectroscopy as shown in Figure S3 in SI. Furthermore, our previous published theoretical calculation (insert of Figure 2d) shown that one of the optimized geometries of Au NCs consisting of 11 Au atoms has only one layer of Au atoms.³ In order to benchmark our results against already available literature, we analyzed published studies on Au NCs containing ~ 10 Au atoms. Although these studies

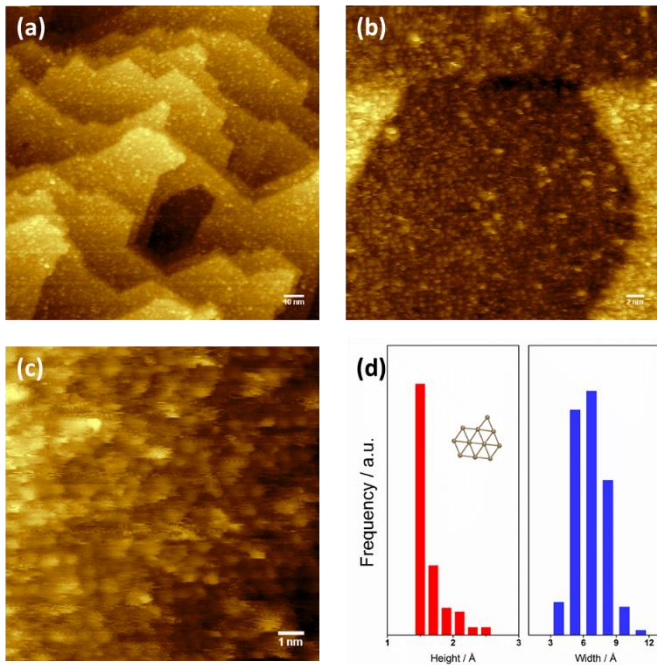


Figure 2: STM images of Au NCs supported on TiO_2 surface and size distribution of Au NCs. (a) to (c): STM images of Au NCs at different magnifications; (d) height and width distribution of Au NCs; insert of (d) shows one of the calculated optimized geometries of Au NCs from our previous work.³

proposed several stable geometries of Au NCs containing ~ 10 Au atoms, one has to be careful in directly comparing them to

our work, given that characterization approaches and synthetic methods described in literature were quite different from ours.^{13-15, 19-22, 30, 40, 41} For example, in one such study, Al Qahtani *et al.* utilized electron microscopy and computational approaches to study structure of Au NCs consisting of 9 Au atoms.²² Although the geometry proposed in Al Qahtani's study was consistent with the model proposed here, it is also important to note that our STM data is more representative of the shape of NCs as compared to that deduced from TEM results.²² Following the STM imaging, the samples were characterized by XPS. Figure 3a shows the Au 4f XPS spectrum of the as-deposited Au NCs. This spectrum could be fitted with only one doublet, indicating a fairly uniform chemical state of Au NCs. The binding energy of Au $4f_{7/2}$ electron was 86.1 eV, which is higher than both the value of 84.0 eV characteristic of bulk Au and the value of 85.6 eV of the precursor gold complex.⁴² Literature analysis indicated that the shift can be explained by different factors, including high oxidation state of clusters, and their small size,^{18, 43} cluster-substrate and cluster-ligand interactions leading to cluster charge.^{16, 17, 22} In our case, the small size effect should be the least significant factor explaining 1.6 eV shift from binding energy of metallic gold, given that the literature described binding energy of Au $4f_{7/2}$ electron of ligand-free Au clusters consisting of only 2 Au atoms was only 84.8 eV.¹⁸ In addition to importance of ligand-cluster interactions to explain the observed shifts, cluster-support interactions should also be considered. For example, published data show 2-D Au NCs consisting of 11 Au atoms would have strong interaction with TiO_2 substrate, resulting in a shift of binding energy of Au $4f_{7/2}$ electron towards higher binding energy.¹⁶ Finally, contribution of high oxidation state of Au should be considered in explaining our data as discussed later in the text.

Following the XPS study of as-deposited Au NCs, the samples were then subjected to different heat treatments to study the evolution of Au NCs. Figure 2 b-d show the Au 4f XPS spectra of Au NCs exposed to heating cycles at 3 discrete temperatures of 373 K, 423 K, and 523 K. The rationale for choosing these temperatures and holding time of 30 min was explained in the experimental method in SI. It can be clearly seen that Au NCs undergo significant evolution upon heat treatment. More specifically, heating the samples at 373 K for 30 min resulted in appearance of new chemical state of Au as indicated by green lines in Figure 3b. In order to account for these states the Au 4f XPS spectrum was fitted with two doublets. The binding energies for Au $4f_{7/2}$ electron were determined to be 86.1 eV and 84.4 eV, indicating a formation of lower binding energy chemical state of Au in addition to higher binding energy component of as-deposited Au NCs. The lower binding energy species might have originated from the partial removal of ligands and/or reduction of as-deposited Au NCs. Further heating of the sample at 423 K for 30 min resulted in complete disappearance of the 86.1 eV doublet as shown in Figure 3c. Such disappearance indicates a complete removal of ligands at this temperature, which is also consistent with published literature.³⁷ Further heating at 523 K for 30 min resulted in appearance of doublet at even lower electron binding energy

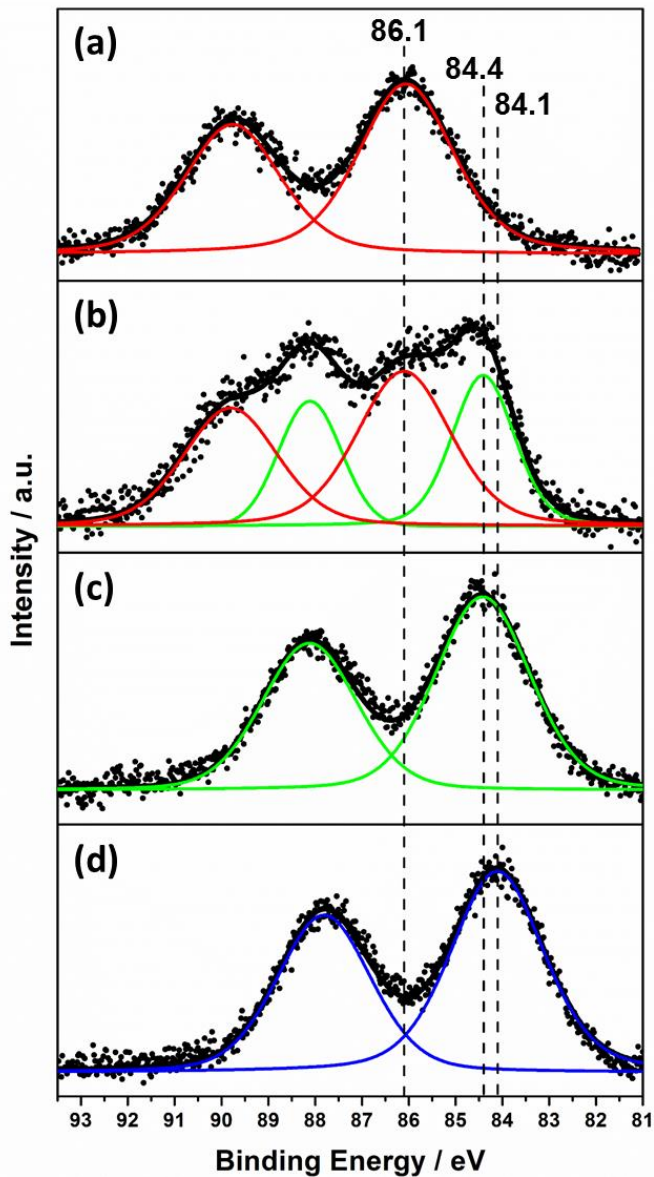


Figure 3: XPS spectra of Au NCs upon different heating treatments. Black dots are experimental data and colored lines represent fitted lines. (a) as-deposited Au NCs; (b) upon heating at 373K; (c) upon heating at 423K; (d) upon heating at 523K. The binding energy of Au 4f_{7/2} electron of different species are indicated by the dash lines.

84.1 eV as indicated by blue line in Figure 3d. Given that this binding energy is very similar to that of bulk Au, it suggests complete reduction of Au species and formation of larger Au particles with properties approaching those of bulk gold. The change in C and P species were also examined. Figure S4 in SI shows the C 1s and P 2p XPS spectra of samples upon heat treatment at different temperatures. No significant changes in C 1s and P 2p spectra as compared to those in Au 4f spectra were observed, indicating that diphosphine ligands remained on the surface after removal from Au cluster. This conclusion also agrees with published study where temperatures higher than 523 K were needed to vaporize the diphosphine ligands.³⁷ STM imaging of samples subjected to heat treatment was also

attempted as a part of our characterization efforts. The STM images of sample heated at 373 K, 423 K, and 523 K are shown in Figure S5 and Figure S6 in SI. Although the image contrast was not sufficient to conduct reliable statistical analysis of size distribution, Au NCs with above-mentioned size and geometry still can be seen in the sample heated at 423 K (Figure S5). Furthermore, the presence of large particles with diameter of ~8.6 nm (Figure S6b and S6d) in the sample heated at 523 K confirmed the formation of larger Au particles with properties approaching those of bulk gold.

The reduction and growth of Au NCs upon heating were then confirmed by *in-situ* XAFS. Figure 4 shows the Au L₃ edge XAFS spectra of as-deposited Au NCs supported on TiO₂ and that of the heat-treated sample, plotted along with the spectrum of standard bulk Au foil. The absorption edge intensity in XANES spectra near the main edge maximum (also known as the white line) is proportional to the empty 5d electron density. In other word, the higher the Au oxidation state, the higher the white line intensity. It can be clearly seen that the heat treatment reduced Au species as the white line intensity decreased toward that of Au foil (Figure 4a). Careful analysis of the spectra revealed that the white line intensity of heated sample was only slightly higher than that of the standard bulk Au foil, indicating that the chemical state of Au species heated up to 523 K was very close to that of bulk Au foil. This observation was also consistent with XPS data (Figure 3d), where the binding energy (84.1 eV) of Au 4f_{7/2} electron was very close to that of bulk Au (84 eV). In the EXAFS region, it can be clearly seen in that the local environment of Au atoms in the as-deposited Au NCs is very different from that in bulk Au foil (Figures 4b). Theoretical fitting results indicate that the average Au-Au coordination number (CN) for the as-deposited Au NCs was 5.4 which is expected for small clusters consisting of ~ 10 atoms.⁴⁴ After heating treatment at 523 K, the local environment of Au atoms in the sample became similar to that in bulk Au foil (Figure 4b). Theoretical fitting results also indicate that the average Au-Au CN increased to 10.6 after heating treatment. Such an increase in Au-Au CN suggests formation of large Au particles, which is consistent with our XPS results. For details of theoretical fitting results of EXAFS data, see Figure S7 and Table S1 in SI. The

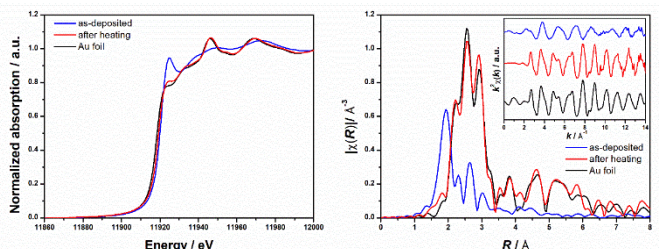


Figure 4: XAFS spectra of Au NCs before and after heating treatment. (a) XANES spectra of as-deposited and heat treated Au NCs along with spectrum of standard bulk Au foil. (b) Fourier transform magnitude of k² weighted EXAFS data of as-deposited and heat treated Au NCs along with those of standard bulk Au foil in R space. Insert of (b) shows the EXAFS data in k space.

overall conclusion from the XAFS analysis, derived from both XANES and EXAFS data, is that the results confirmed the

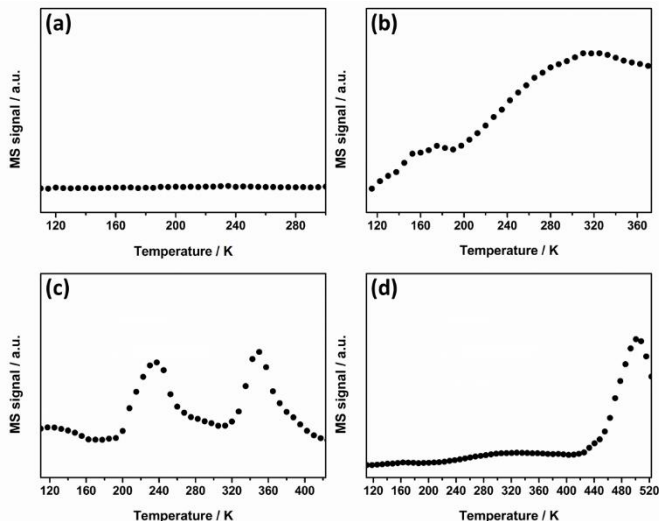


Figure 5: TPD results of CO oxidation over Au NCs upon different heating treatments. The “m/e=45” signals representing the production of $^{13}\text{CO}_2$ are shown here. (a) as-deposited Au NCs; (b) upon heating at 373 K; (c) upon heating at 423 K; (d) upon heating at 523 K.

reduction and growth of Au NCs upon heating in line with the XPS and STM results.

In order to evaluate catalytic activity of heat treated Au NCs, CO oxidation TPD experiments were conducted for samples treated at several different temperatures. The upper temperatures for corresponding TPD experiments were set to be the same as the heat treatment temperatures. Figure 5 displays the TPD results for CO_2 ($^{13}\text{CO}_2$, $m/z = 45$) originating from CO oxidation on as-deposited and heat treated samples. The as-deposited Au NCs did not show CO oxidation activity within 110 K to 300 K temperature range. This result was consistent with reports showing the absence of CO oxidation activity up to temperatures of 473 K^{45, 46} on ligand-protected Au clusters deposited on TiO_2 . In contrast to as-deposited NCs, the samples heated at 373 K for 30 min exhibited CO oxidation activity (Figure 5b). The broad feature at 130 - 373 K temperature range in Figure 5b indicates a presence of more than one active site for CO_2 formation and/or reaction pathway as described below. Importantly, the activity of NCs for CO oxidation coincides with onset of ligand removal, as deduced from XPS results discussed earlier. Further heating at 423 K resulted in several well-defined TPD features (Figure 5c). These features include two distinct peaks at 200 K and 330 K indicating two different active sites for CO_2 formation and/or reaction pathways. Figure 5d shows the TPD results for sample treated at 523 K. The low temperature CO_2 desorption peak shown in Figure 5c disappeared from the TPD spectrum shown in Figure 5d, with appearance of high temperature CO_2 desorption peak starting at 430 K. In order to explain these results, it is important to correlate this data to the one in published literature. More specifically, the published literature describes several CO oxidation reaction pathways over TiO_2 supported Au catalysts,⁴⁷⁻⁵¹ with a particular emphasis being placed on different origins of active oxygen species. For example, recently Widmann *et al.* suggested that the active oxygen species at low temperature CO oxidation are originated

from the absorbed molecular oxygen while those at high temperature originated from lattice oxygen in the support oxide.⁵² In both cases, the Au/ TiO_2 interface plays an important role. As described in literature, at low temperature (typically below 150 K), molecular oxygen is adsorbed and activated at the perimeter of Au/ TiO_2 interface. Subsequently, CO adsorbed on either Au or TiO_2 can react with activated oxygen to form CO_2 .^{49, 50} In contrast to low temperature scenario of dissociated oxygen, at high temperature (typically above 353 K), the lattice oxygen atoms located at the perimeter of Au/ TiO_2 interface can react with CO adsorbed on Au.⁵³ As a result of this reaction, oxygen vacancies are generated following desorption of CO_2 and replenished through interaction with oxygen gas.^{47, 48, 53} It is important to highlight several other differences in reaction pathways at low and high temperatures. While CO_2 formation from CO is considered to be the only reaction pathway at low temperature,⁴⁹ formation of other species, such as carbonates and bicarbonates has been reported to take place at high temperature.^{53, 54} Carbonate-like species have been proposed as important CO oxidation intermediates, which then can form CO_2 at higher temperature.⁵³⁻⁵⁵ Given the pathways described above, our results indeed indicate different pathways for CO oxidation at different temperatures. The low temperature CO_2 desorption peak starting at 200 K (Figure 5c) corresponds to CO_2 formation and desorption resulting from activated molecular oxygen pathway. In contrast, the high temperature CO_2 desorption peak starting at 330 K corresponds to formation and desorption of CO_2 resulting from activated lattice oxygen pathway involving either a direct formation of CO_2 and/or indirect formation via decomposition of carbonate-like species. Meanwhile, the disappearance of low temperature CO_2 desorption peak during the sample heating up to 523 K (Figure 5d) indicates that the ability of Au/ TiO_2 to catalyze CO_2 oxidation through the activated molecular oxygen pathway was inhibited due to high temperature sample treatment. Furthermore, the shift of high temperature CO_2 desorption peak (Figure 5d) from 330 K to 430 K indicates possible formation of various carbonate-like species which was confirmed by XPS (Figure S8), that decompose and form CO_2 at higher temperature than that encountered during the direct CO oxidation through the activated lattice oxygen pathway. In addition to role of oxygen to explain various pathways of CO_2 formation, it is also important to highlight the importance of ligand removal for Au NCs activation. As shown in Figure 5a, the as-deposited Au NCs did not exhibit CO oxidation activity, indicating that the ligands probably inhibit the interfacial chemistry of Au/ TiO_2 for both low and high temperature oxygen activation pathways, such as molecular oxygen and lattice oxygen atoms mechanisms respectively. The ligands might also prevent CO adsorption and activation.⁵⁶⁻⁵⁸ The importance of Au NPs deprotection to oxidize CO has been examined in a recent study by Wu *et al.*, which indicated that Au NCs containing 22 Au atoms protected by similar diphosphine ligands had mild CO oxidation activity, although the authors also implied that not all the atoms in the NCs were coordinated with ligands and that such uncoordinated Au atoms are essential for catalyzing CO oxidation.³⁷ In our case, considering that NCs contained around

10 Au atoms, almost every Au atom was coordinated to ligand and thereby exhibited no catalytic activity for CO oxidation. Furthermore, considering the diphosphine ligands possibly stayed on the surface after heat treatments (Figure S4 and discussion above), the observed activity of Au NCs for CO oxidation indicated that deprotection of Au NCs was probably more critical than other factors for catalytic application of Au NCs. Given all the above mentioned, it is plausible to suggest that removal of ligands is a necessary step to activate Au NCs for CO oxidation.

Conclusions

In conclusion, we successfully synthesized Au NCs through a ligand exchange approach. Detailed characterizations were carried out to study the morphology and electronic properties of these Au NCs. The impact of heat treatment on Au NCs was examined by XPS, *in-situ* XAFS, and CO oxidation TPD techniques. We have showed that removal of ligands by heat treatment at intermediate temperatures is a critical step to activate very small Au NCs to induce their catalytic activity. However, high temperatures can result in coarsening of Au NCs to form bulk-like large particles, which exhibit lower catalytic activity for CO oxidation as compared to that for smaller particles.

Conflicts of interest

There are no conflicts to declare.

Acknowledgements

We acknowledge funding support from the National Science Foundation (#1254600). We acknowledge the support from the U.S. Department of Energy Grant No. DE-FG02-03ER15476 and Synchrotron Catalysis Consortium (U.S. Department of Energy, Office of Basic Energy Sciences, Grant No. DE-SC0012335). This research used resources of the Center for Functional Nanomaterials, which is a U.S. DOE Office of Science Facility, at Brookhaven National Laboratory under Contract No. DE-SC0012704. We thank Dr. Mintcho Tikhov from Cambridge University for helpful discussion.

Notes and references

- Y. Lu and W. Chen, *Chemical Society Reviews*, 2012, **41**, 3594-3623.
- S. Zhao, G. Ramakrishnan, D. Su, R. Rieger, A. Koller and A. Orlov, *Applied Catalysis B: Environmental*, 2011, **104**, 239-244.
- P. Shen, S. Zhao, D. Su, Y. Li and A. Orlov, *Applied Catalysis B: Environmental*, 2012, **126**, 153-160.
- Q. Wu, S. Xiong, P. Shen, S. Zhao, Y. Li, D. Su and A. Orlov, *Catalysis Science & Technology*, 2015, **5**, 2059-2064.
- Y. Lei, F. Mehmood, S. Lee, J. Greeley, B. Lee, S. Seifert, R. E. Winans, J. W. Elam, R. J. Meyer and P. C. Redfern, *Science*, 2010, **328**, 224-228.
- R. Siburian, T. Kondo and J. Nakamura, *The Journal of Physical Chemistry C*, 2013, **117**, 3635-3645.
- G. C. Bond, P. A. Sermon, G. Webb, D. A. Buchanan and P. B. Wells, *Journal of the Chemical Society, Chemical Communications*, 1973, DOI: 10.1039/C3973000444B, 444b-445.
- M. Haruta, T. Kobayashi, H. Sano and N. Yamada, *Chemistry Letters*, 1987, 405-408.
- M. Okumura, S. Nakamura, S. Tsubota, T. Nakamura, M. Azuma and M. Haruta, *Catalysis Letters*, 1998, **51**, 53-58.
- U. Landman, B. Yoon, C. Zhang, U. Heiz and M. Arenz, *Topics in Catalysis*, 2007, **44**, 145-158.
- S. Lee, C. Fan, T. Wu and S. L. Anderson, *Journal of the American Chemical Society*, 2004, **126**, 5682-5683.
- X. Tang, J. Schneider, A. Dollinger, Y. Luo, A. S. Worz, K. Judai, S. Abbet, Y. D. Kim, G. F. Gantefor, D. H. Fairbrother, U. Heiz, K. H. Bowen and S. Proch, *Physical Chemistry Chemical Physics*, 2014, **16**, 6735-6742.
- F. Wen, U. Englert, B. Gutrat and U. Simon, *European Journal of Inorganic Chemistry*, 2008, **2008**, 106-111.
- Y. Shichibu, K. Suzuki and K. Konishi, *Nanoscale*, 2012, **4**, 4125-4129.
- J. F. Alvino, T. Bennett, D. Anderson, B. Donoeva, D. Ovoshchnikov, R. H. Adnan, D. Appadoo, V. Golovko, G. Andersson and G. F. Metha, *RSC Advances*, 2013, **3**, 22140-22149.
- D. P. Anderson, J. F. Alvino, A. Gentleman, H. A. Qahtani, L. Thomsen, M. I. J. Polson, G. F. Metha, V. B. Golovko and G. G. Andersson, *Physical Chemistry Chemical Physics*, 2013, **15**, 3917-3929.
- D. P. Anderson, R. H. Adnan, J. F. Alvino, O. Shipper, B. Donoeva, J.-Y. Ruzicka, H. Al Qahtani, H. H. Harris, B. Cowie, J. B. Aitken, V. B. Golovko, G. F. Metha and G. G. Andersson, *Physical Chemistry Chemical Physics*, 2013, **15**, 14806-14813.
- S. Peters, S. Peredkov, M. Neeb, W. Eberhardt and M. Al-Hada, *Surface Science*, 2013, **608**, 129-134.
- J. Chen, Q.-F. Zhang, T. A. Bonaccorso, P. G. Williard and L.-S. Wang, *Journal of the American Chemical Society*, 2014, **136**, 92-95.
- F. Dufour, B. Fresch, O. Durupthy, C. Chaneac and F. Remacle, *The Journal of Physical Chemistry C*, 2014, **118**, 4362-4376.
- L. Yang, H. Cheng, Y. Jiang, T. Huang, J. Bao, Z. Sun, Z. Jiang, J. Ma, F. Sun, Q. Liu, T. Yao, H. Deng, S. Wang, M. Zhu and S. Wei, *Nanoscale*, 2015, **7**, 14452-14459.
- H. S. Al Qahtani, K. Kimoto, T. Bennett, J. F. Alvino, G. G. Andersson, G. F. Metha, V. B. Golovko, T. Sasaki and T. Nakayama, *The Journal of Chemical Physics*, 2016, **144**, 114703.
- H. S. Al Qahtani, G. F. Metha, R. B. Walsh, V. B. Golovko, G. G. Andersson and T. Nakayama, *The Journal of Physical Chemistry C*, 2017, **121**, 10781-10789.
- B. C. Gates, *Chemical Reviews*, 1995, **95**, 511-522.
- H. Li, L. Li and Y. Li, *Nanotechnology Reviews*, 2013, **2**, 515-528.
- P. D. Jazdzinsky, G. Calero, C. J. Ackerson, D. A. Bushnell and R. D. Kornberg, *Science*, 2007, **318**, 430-433.
- Z. Y. Li, N. P. Young, M. Di Vece, S. Palomba, R. E. Palmer, A. L. Bleloch, B. C. Curley, R. L. Johnston, J. Jiang and J. Yuan, *Nature*, 2008, **451**, 46-48.

28. S. Mostafa, F. Behafarid, J. R. Croy, L. K. Ono, L. Li, J. C. Yang, A. I. Frenkel and B. R. Cuenya, *Journal of the American Chemical Society*, 2010, **132**, 15714-15719.

29. Q. Wu, C. J. Ridge, S. Zhao, D. Zakharov, J. Cen, X. Tong, E. Connors, D. Su, E. A. Stach, C. M. Lindsay and A. Orlov, *The Journal of Physical Chemistry Letters*, 2016, **7**, 2910-2914.

30. H. Yao and M. Iwatsu, *Langmuir*, 2016, **32**, 3284-3293.

31. M. F. Bertino, Z.-M. Sun, R. Zhang and L.-S. Wang, *The Journal of Physical Chemistry B*, 2006, **110**, 21416-21418.

32. B. Yoon, H. Häkkinen, U. Landman, A. S. Wörz, J.-M. Antonietti, S. Abbet, K. Judai and U. Heiz, *Science*, 2005, **307**, 403-407.

33. X. Tong, L. Benz, P. Kemper, H. Metiu, M. T. Bowers and S. K. Buratto, *Journal of the American Chemical Society*, 2005, **127**, 13516-13518.

34. L. Benz, X. Tong, P. Kemper, H. Metiu, M. T. Bowers and S. K. Buratto, *The Journal of Physical Chemistry B*, 2006, **110**, 663-666.

35. M. Turner, V. B. Golovko, O. P. H. Vaughan, P. Abdulkin, A. Berenguer-Murcia, M. S. Tikhov, B. F. G. Johnson and R. M. Lambert, *Nature*, 2008, **454**, 981-983.

36. G. G. Andersson, V. B. Golovko, J. F. Alvino, T. Bennett, O. Wrede, S. M. Mejia, H. S. A. Qahtani, R. Adnan, N. Gunby, D. P. Anderson and G. F. Metha, *The Journal of Chemical Physics*, 2014, **141**, 014702.

37. Z. Wu, G. Hu, D.-e. Jiang, D. R. Mullins, Q.-F. Zhang, L. F. Allard, L.-S. Wang and S. H. Overbury, *Nano Letters*, 2016, **16**, 6560-6567.

38. H. Onishi and Y. Iwasawa, *Surface Science*, 1994, **313**, L783-L789.

39. U. Diebold, J. F. Anderson, K.-O. Ng and D. Vanderbilt, *Physical Review Letters*, 1996, **77**, 1322-1325.

40. J. M. Pettibone, W. A. Osborn, K. Rykaczewski, A. A. Talin, J. E. Bonevich, J. W. Hudgens and M. D. Allendorf, *Nanoscale*, 2013, **5**, 6558-6566.

41. C. C. Chusuei, X. Lai, K. A. Davis, E. K. Bowers, J. P. Fackler and D. W. Goodman, *Langmuir*, 2001, **17**, 4113-4117.

42. Y. M. Shul'ga, A. V. Bulatov, R. A. T. Gould, W. V. Konze and L. H. Pignolet, *Inorganic Chemistry*, 1992, **31**, 4704-4706.

43. P. M. T. M. Van Attekum, J. W. A. Van der Velden and J. M. Trooster, *Inorganic Chemistry*, 1980, **19**, 701-704.

44. A. I. Frenkel, L. D. Menard, P. Northrup, J. A. Rodriguez, F. Zypman, D. Glasner, S. P. Gao, H. Xu, J. C. Yang and R. G. Nuzzo, *AIP Conference Proceedings*, 2007, **882**, 749-751.

45. X. Nie, H. Qian, Q. Ge, H. Xu and R. Jin, *ACS Nano*, 2012, **6**, 6014-6022.

46. G. Li and R. Jin, *Accounts of Chemical Research*, 2013, **46**, 1749-1758.

47. D. Widmann and R. J. Behm, *Angewandte Chemie International Edition*, 2011, **50**, 10241-10245.

48. D. Widmann and R. J. Behm, *Accounts of Chemical Research*, 2014, **47**, 740-749.

49. I. X. Green, W. Tang, M. Neurock and J. T. Yates, *Science*, 2011, **333**, 736-739.

50. I. X. Green, W. Tang, M. Neurock and J. T. Yates, *Accounts of Chemical Research*, 2014, **47**, 805-815.

51. Y.-G. Wang, D. C. Cantu, M.-S. Lee, J. Li, V.-A. Glezakou and R. Rousseau, *Journal of the American Chemical Society*, 2016, **138**, 10467-10476.

52. D. Widmann, A. Krautsieder, P. Walter, A. Brückner and R. J. Behm, *ACS Catalysis*, 2016, **6**, 5005-5011.

53. Y. Denkowitz, Z. Zhao, U. Hörmann, U. Kaiser, V. Plzak and R. J. Behm, *Journal of Catalysis*, 2007, **251**, 363-373.

54. P. Konova, A. Naydenov, C. Venkov, D. Mehandjiev, D. Andreeva and T. Tabakova, *Journal of Molecular Catalysis A: Chemical*, 2004, **213**, 235-240.

55. C. K. Costello, M. C. Kung, H. S. Oh, Y. Wang and H. H. Kung, *Applied Catalysis A: General*, 2002, **232**, 159-168.

56. Z. Wu, D.-e. Jiang, A. K. P. Mann, D. R. Mullins, Z.-A. Qiao, L. F. Allard, C. Zeng, R. Jin and S. H. Overbury, *Journal of the American Chemical Society*, 2014, **136**, 6111-6122.

57. L. D. Menard, F. Xu, R. G. Nuzzo and J. C. Yang, *Journal of Catalysis*, 2006, **243**, 64-73.

58. S. Gaur, J. T. Miller, D. Stellwagen, A. Sanampudi, C. S. S. R. Kumar and J. J. Spivey, *Physical Chemistry Chemical Physics*, 2012, **14**, 1627-1634.